# Characterization of composite cellulosic separators for rechargeable lithium-ion batteries

Isao Kuribayashi

*Asahi Chemical Industry Co., Ltd., 1-1-2 Yuraku-cho, Chiyoda-ku, Tokyo 100, Japan*

## Abstract

Thin composite cellulosic separators (39–85 μm thickness), composed of fine fibrilliform cellulosic fibres (diameter 0.5 to 5.0 μm) embedded in microporous (pore diameter: 10–200 nm) cellulosic film and soaked in ethylene carbonate or other aprotic solvent, are found to possess fair-to-moderate physical strength, an apparent complete freedom from pinholes, and a complex impedance equal to or lower than that of conventional polyolefin separators for rechargeable lithium-ion batteries. Laboratory-scale cells that comprise $LiCoO_2$/petroleum coke electrodes, 1.0 M $LiBF_4$/PC:EC:BL (25:25:50 by volume; propylene carbonate:ethylene carbonate:γ-butyrolactone) electrolyte and the cellulosic separators exhibit good initial discharge capacity and capacity retention over 41 charge/discharge cycles. The latter are indistinguishable from those obtained from a similar cell with conventional polyolefin separator.

*Keywords:* Cellulosic separators; Lithium-ion cells; Rechargeable batteries

## 1. Introduction

Rechargeable lithium-ion batteries (LIBs) for portable electronic equipment have generally employed polyolefin separators since the time of their initial development. This has been partly because the characteristics and performance of aprotic solvents in small primary lithium cells with polyolefin separators have been known for many years and this knowledge base was readily applicable to LIBs.

If LIBs are to be employed in future applications such as load-levelling systems at electric power plants or lightweight electric vehicles, the possibility of heat evolution that could lead to separator meltdown in the event of internal short-circuiting or overcharging must be considered; other separators may therefore be preferable.

Electrolytic paper has long been employed in electrolytic capacitors with aprotic solvents such as γ-butyrolactone (BL), but a literature search [1] reveals no previous investigation of the use of cellulosic fibre separators for lithium or lithium-ion batteries. This apparent lack of interest may be related to the hygroscopic nature of cellulosic papers and films, their tendency to degrade in contact with lithium metal, and their susceptibility to pinhole formation at thicknesses of less than 100 μm.

An exploratory investigation has therefore commenced in the author's laboratory to determine the requirements and

possibility of developing cellulosic separators for LIBs. Pristine electrolytic paper displays little $Li^+$ ion conductivity with the electrolyte 1 M $LiBF_4$/PC:EC:BL (25:25:50 by volume) normally employed in LIBs. The conductivity improves somewhat when the paper is first treated by pounding to increase the fibrilliform content, but this also reduces the mechanical strength.

In an attempt to obtain an acceptable balance of $Li^+$ ion conductivity, mechanical strength, and resistance to pinhole formation, composite separators that consist of fibrilliform cellulosic fibres embedded in a microporous cellulosic film have been fabricated. The physical and chemical characteristics and performance of these fibres have been evaluated in an $Li^+$ test cell.

## 2. Experimental

Five composite cellulosic separators were jointly fabricated and supplied for this study by Nippon Kodoshi Corporation and Tomiyama Pure Chemical Industry; they were used as received, and denoted: CX-1EC, CX-2EC, CX-3EC, CX-3PC, and CX-3BL (EC, PC, and BL indicate impregnating with ethylene carbonate, propylene carbonate, and γ-butyrolactone, respectively, during separator fabrication). The electrolytic papers ME4-20 and MR5D1-50 and the

polypropylene (PP) separator were all commercially available products.

The number of pinholes in the separators, as received, was determined by observation with a Toyobo Image Analyzer V10 and calculated as the average number of pinholes larger than $1 \times 10^{-4}$ mm$^2$ in the observed area of 81.3 mm$^2$. High-resolution secondary electron micrographs were obtained with a JOEL JSM-6320F field emission–scanning transmission electron microscope (FE–SEM).

All liquid electrolytes and the mixed solvent PC:EC:BL (25:25:50 by volume) were obtained from Tomiyama Pure Chemical Industry and used as received. The guaranteed water content was less than 20 ppm.

Total conductivity (taken as ion conductivity in all except the preliminary investigation) was measured by the standard a.c. impedance method in a frequency range of 20 Hz to 1 MHz, with a Hewlett-Packard 4284A precision LCR meter and electrodes that consisted of two parallel copper disks of thickness 0.50 mm and diameter 10.0 mm. In the preliminary investigation, the electronic conductivity was measured by the two-terminal method with a voltage of 100 mV d.c. across the copper disk electrodes, and an Advantest R8340A ultra-high resistance meter.

Complex impedance for the Cole–Cole plots was measured by the two-terminal method, with the same LCR meter and electrodes that comprised the same copper disks covered with freshly scraped lithium metal foil, and a signal of 10 mV applied across the sample.

Cells were fabricated by securing a positive electrode sheet (10 mm × 15 mm), a separator (13 mm × 18 mm), and a negative electrode sheet (11 mm × 16 mm) between glass plates with a metal clip and immersing the assembly in the indicated electrolyte. The cell capacity, expressed as mAh per g of active material within the region of the electrodes overlap (10 mm × 15 mm), was measured electrochemically with a Hokutodenko Model HJ-101SM6 charge/discharge unit and the related SCB-01A program was employed for charge/discharge data processing and chart drawing.

All conductivity measurements were made at 25 °C, and measurement samples were packed in airtight glass vessels and handled in an argon gas flow glove box, to prevent moisture absorption.

## 3. Results and discussion

### 3.1. Preliminary comparison of ionic and electronic conductivity with copper electrodes

Copper current-collectors are commonly employed in rechargeable lithium-ion batteries, and copper electrodes were therefore used throughout the present study, rather than the stainless-steel electrodes that are conventionally used for measurement of electronic conductivity. Preliminary investigation showed that the copper electrodes were appropriate for this purpose. The microporous PP separator soaked in 1.0 M LiBF$_4$/PC:EC:BL solution exhibited an electronic conductivity of $1.5 \times 10^{-9}$ S cm$^{-1}$ and a total conductivity of $0.7 \times 10^{-3}$ S cm$^{-1}$. When soaked in the mixed solvent PC:EC:BL containing no lithium salt, its electronic conductivity was $1.5 \times 10^{-9}$ S cm$^{-1}$ and its total conductivity was $0.8 \times 10^{-5}$ S cm$^{-1}$. These results showed that the electronic conductivity with the copper electrodes was negligible, and the total conductivity was therefore taken as representing the ion conductivity throughout the remainder of this study.

### 3.2. Physical characteristics and structure of separators

The physical properties of the composite cellulosic separators CX-1EC, CX-2EC, and CX-3EC are shown in Table 1, together with those of the commercially available electrolytic paper (ME4-20 and MR5D1-50) and PP separators. The three composite cellulosic separators had been impregnated with EC during their preparation, but neither they nor the electrolytic papers or PP separator had yet been immersed in the mixed-solvent electrolyte. No pinholes were found in any of the CX-series separators.The tensile strength of both CX-1EC and CX-3EC was above the minimum believed necessary for practical utilization in lithium-ion batteries, but that of CX-2EC was unacceptably low.

The microstructures of the three EC-infused CX-series separators are shown in Figs. 1–3, and that of the electrolytic paper MR5D1-50 (with no EC impregnation) is provided for comparison on Fig. 4. In all three CX-series separators, the dark areas between the fibres represent the cellulosic film matrix. As shown by the FE–SEM micrographs of CX-3EC

Table 1

Physical characteristics of three composite cellulosic separators impregnated with ethylene carbonate (CX-1EC, CX-2EC, CX-3EC), in comparison with pounded-fibre electrolytic papers (ME4-20 and MR5D1-50) and conventional microporous polypropylene (PP) separator. All measurements made prior to soaking in electrolyte

| | Basis weight (g m$^{-2}$) | Density (g m$^{-3}$) | Air permeability (s per 100 cm$^3$) | Tensile strength [a] (kg cm$^{-2}$) | Elongation (%) | Number of pin holes |
|---|---|---|---|---|---|---|
| CX-1EC | 16.0 | 0.53 | >3000 | 53 | 20 | 0 |
| CX-2EC | 8.9 | 0.95 | >3000 | 2 | 6 | 0 |
| CX-3EC | 8.5 | 0.62 | >3000 | 85 | 20 | 0 |
| ME4-20 | 15.0 | 0.74 | >3000 | 830 | 3.5 | 3 |
| MR5D1-50 | 21.6 | 0.43 | 2.9 | 340 | 3.5 | 183 |
| PP separator | 14.4 | 0.58 | >3000 | 1010 | 140 | 0 |

[a] As measured with 2.5 cm span, 20 cm/min cross-head speed.

Fig. 1. SEM micrograph of CX-1EC separator, fabricated by matting cellulosic fibres (average diameter ~5 μm) and embedding mat in cellulosic film followed by impregnation with ethylene carbonate.
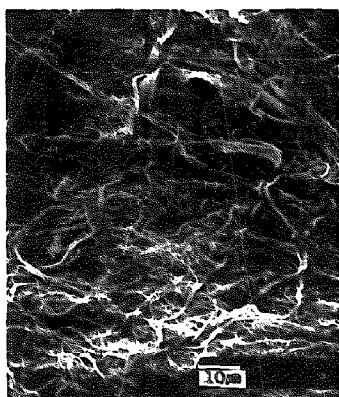


Fig. 2. SEM micrograph of CX-2EC separator, fabricated from a slurry of cellulose fibres (average diameter ~0.5 μm) in a cellulose solution followed by impregnation with ethylene carbonate.
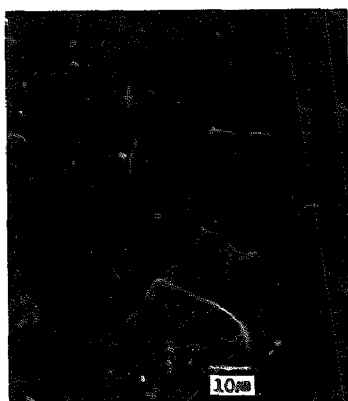


Fig. 3. SEM micrograph of CX-3EC separator, fabricated by matting cellulosic fibres (average diameter ~0.5 μm) and embedding mat in a cellulosic film followed by impregnation with ethylene carbonate.

in Fig. 5 (magnification, ×10⁵) and in Fig. 6 (magnification, ×2×10⁵), in which the EC has been removed by vacuum evaporation to permit the FE–SEM observation, the cellulosic film in all three composite cellulosic separators was characterized by a microporous structure, with pore diameters in the range 10 to 200 nm.

The differing structures of the three CX-series membranes (evident in Figs. 1–3), as well as their differing physical properties (Table 1), reflect their different methods of fabrication. All three were obtained from pre-pounded, fibrilliform cellulosic fibres, but the average starting diameter of the fibre in CX-1EC was ~5 μm, while that in CX-2EC and CX-3EC was an order of magnitude smaller, i.e., ~0.5 μm. In
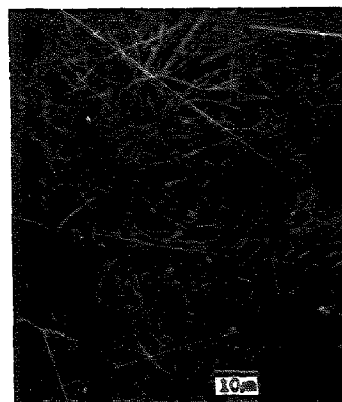


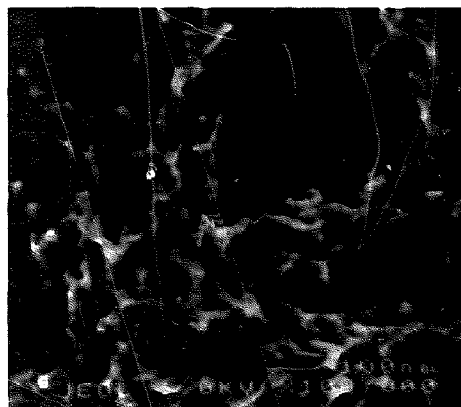Fig. 4. SEM micrograph of electrolytic paper MR5D1-50, fabricated from pounded fibres (average diameter ~10 μm).



Fig. 5. FE–SEM micrograph of CX-3EC separator following removal of its ethylene carbonate by vacuum evaporation, magnification, ×10⁵.



Fig. 6. FE–SEM micrograph of CX-3EC separator following removal of its ethylene carbonate by vacuum evaporation, magnification: ×2×10⁵.

CX-1EC and CX-3EC, moreover, the fibres were first formed into a web and then embedded in the cellulosic film matrix, while the web and matrix were formed concurrently in CX-2EC. The apparent thickness of the CX-2EC fibres (as seen in Fig. 2) may be the result of a strong tendency for fibre intertwining or aggregation during the concurrent fibre matting and film embedding process used to fabricate the membrane.

### 3.3. Ion conductivity and complex impedance

As shown in Table 2, all three of the CX-series separators, following soaking in the 1.0 M LiBF₄/PC:EC:BL (25:25:50) mixed solvent, exhibited lithium-ion conductivities somewhat higher than that of the PP separator at both 1 kHz and 500 kHz. Among the three composite cellulosic separators, the conductivities were highest with CX-1EC, intermediate with CX-2EC, and lowest with CX-3EC.

In the Cole–Cole plots of the complex impedance, however, the CX-3EC separator exhibited substantially lower impedance than the CX-1EC separator, which was nearly the same as that of the PP separator, and the CX-2EC separator, which was intermediate (see Fig. 7). The Cole–Cole plot is a closer predictor of the performance of the separator in an



Fig. 8. Cole–Cole plots of complex impedance of CX-3EC, CX-3PC, and CX-3BL composite cellulosic separators after soaking in 1.0 M LiBF₄/PC:EC:BL (25:25:50), between lithium electrodes. Impregnated aprotic solvents: ethylene carbonate (EC), propylene carbonate (PC), and γ-butyrolactone (BL).

actual lithium-ion cell, and on the basis of this result as well as the superior physical characteristics of the CX-3EC separator, the CX-3 composite was selected as the main object of investigation in the experiments with other aprotic solvents and fabricated cells, as described below.

### 3.4. Complex impedance of CX-3 composite with other aprotic solvents

Composite separators CX-3PC and CX-3BL were fabricated in the same manner as CX-3EC, except for immersion in PC and BL, respectively, rather than in EC. Each separator was then soaked in the 1 M LiBF₄/PC:EC:BL (25:25:50) mixed solvent, as described above, and Cole–Cole plots of the complex impedance were obtained. As shown in Fig. 8, the results are nearly the same with all three aprotic solvents. This suggests that the composite cellulosic separator may well be amenable to a relatively broad selection of aprotic solvents and thus permits flexibility in the future development and design of lithium-ion cells that incorporates such separators.

Table 2
Lithium-ion conductivity and thickness of three cellulosic separators impregnated with ethylene carbonate (CX-1EC, CX-2EC, CX-3EC), in comparison with pounded-fibre electrolytic papers (ME4-20 and MR5D1-50) and conventional microporous polypropylene (PP) separator, all after soaking in 1.0 M LiBF₄/PC:EC:BL (25:25:50)

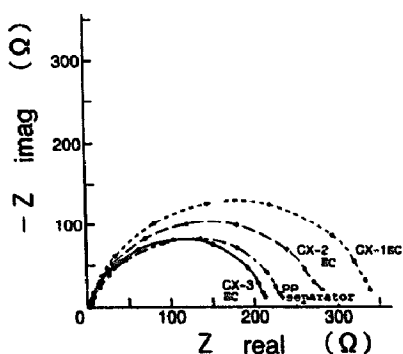| | Thickness (μm) | Ion conductivity ($\times 10^{-3}$ S cm$^{-1}$) | |
|---|---|---|---|
| | | 1 kHz | 500 kHz |
| CX-1EC | 47 | 1.2 | 3.1 |
| CX-2EC | 85 | 0.8 | 2.6 |
| CX-3EC | 39 | 0.4 | 2.0 |
| ME4-20 | 21 | 0.07 | 0.04 |
| MR5D1-50 | 51 | 0.4 | 1.2 |
| PP separator | 25 | 0.2 | 0.7 |

### 4. Performance in test cells

For experimental-scale lithium-ion cells that comprised a LiCoO₂ positive electrode, a petroleum coke negative electrode, and a 1 M LiBF₄/PC:EC:BL (25:25:50) electrolyte, the cell performance with the composite cellulosic separators CX-1EC, CX-2EC, and CX-3EC was practically indistinguishable from that with the conventional polyethylene separator. In all four cases, the cells showed an initial discharge capacity of approximately 78 mAh g$^{-1}$ and a final discharge capacity of approximately 62 mAh g$^{-1}$ after 41 charge/discharge cycles between 4.20 and 2.70 V, see Fig. 9. In all cases, the gradual decrease in discharge capacity was largely attributable to capacity fading of the LiCoO₂ electrode.



Fig. 7. Cole–Cole plots of complex impedance of three composite cellulosic separators (CX-1EC, CX-2EC, CX-3EC) and polypropylene (PP) separator after soaking in 1.0 M LiBF₄/PC:EC:BL (25:25:50), between lithium electrodes.
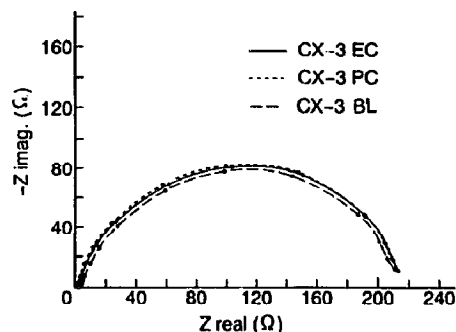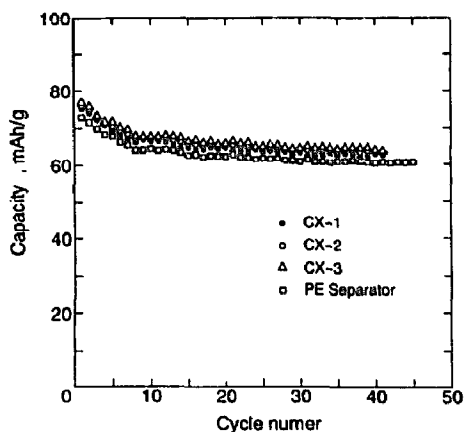
Fig. 9. Cycling behaviour of CX-1EC, CX-2EC, and CX-3EC composite cellulosic separators and conventional polyethylene separator, in cells containing $LiCoO_2$/petroleum coke electrodes and 1 M $LiBF_4$/PC:EC:BL (25:25:50) electrolyte, with charge/discharge between 4.20 and 2.70 V.

## 5. Conclusions

Composite cellulosic separators that consist of fibrilliform cellulosic fibres embedded in a microporous cellulosic matrix soaked in an aprotic solvent provide a promising alternative to polyolefin separators in the future development of rechargeable lithium-ion batteries. The fibres reduce the possibility of separator meltdown under exposure to heat generated by overcharging or internal short-circuiting in applications such as load-levelling at electric power plants or lightweight electric vehicles. It is planned to conduct further investigations on the performance of these separators in cell systems based on lithium/manganese oxides and carbons.

## Reference

[1] Dialog Files: *No. 399 CA Search 67-, No. 302 Kirk-Othmer Online, No. 2 INSPEC 69-, No. 6 NITIS and No. 8 EiCOMPENDEX PLUS.*